Hydrodynamic focusing in microstructures: Improved detection efficiencies in subfemtoliter probe volumes

Cite as: J. Appl. Phys. **101**, 084903 (2007); https://doi.org/10.1063/1.2721752
Submitted: 04 November 2006 . Accepted: 27 February 2007 . Published Online: 17 April 2007

Andrew J. de Mello, and Joshua B. Edel

Hydrodynamic focusing in microstructures: Improved detection efficiencies in subfemtoliter probe volumes

Andrew J. de Mello[a)]
Department of Chemistry, Imperial College London, Exhibition Road, South Kensington, London SW7 2AZ, United Kingdom

Joshua B. Edel[b)]
Department of Chemistry, Imperial College London, Exhibition Road, South Kensington, London SW7 2AZ, United Kingdom and Institute of Biomedical Engineering, Imperial College London, Exhibition Road, South Kensington, London SW7 2AZ, United Kingdom

(Received 4 November 2006; accepted 27 February 2007; published online 17 April 2007)

We present a method for improving detection efficiencies in single molecule confocal fluorescence spectroscopy with subfemtoliter probe volumes within microfluidic channels. Our approach is based on hydrodynamically focusing an analyte stream within a microfluidic channel down to a width on the same order of magnitude as that of the confocal probe volume. Experiments are performed in which fluorescently labeled polystyrene microspheres (930 nm diameter) are motivated through a microchannel and passed through a focused laser beam at a variety of flow rates (0.1 -11 μL/min). Hydrodynamic focusing of the analyte stream is achieved by introduction of two sheath flow streams that flank the central analyte stream. Through variation of the relative flow rates in each input stream the analyte stream can be controlled with micron resolution. A maximum hydrodynamic focusing width of 3 μm was achieved within a 50 μm wide microfluidic channel; hence, a larger proportion of molecules traveling through the microfluidic device were detected. Furthermore, simple statistical methods are used to investigate the resulting fluorescence bursts and generate single-particle burst width and burst area distributions. From these data, the total detection efficiencies are shown to be an order of magnitude better than those achievable in conventional unfocused systems. © *2007 American Institute of Physics*. [DOI: 10.1063/1.2721752]

I. INTRODUCTION

In recent years, the study of single molecules and particles within flowing streams has received much attention in biological research, with applications in fields such as nucleic acid analysis, gene expression, and DNA sequencing.[1,2] A number of distinct approaches have been proposed in order to detect single molecules and particles in solution, with most incorporating the measurement of absorption or emission processes.[3–8] The most popular of these methods is based on confocal fluorescence spectroscopy (CFS).[2–5] Typically, a femtoliter probe volume is defined by a laser beam focused to a diffraction limited spot using a high numerical aperture objective. As a molecule traverses the laser beam it is repeatedly cycled between ground and excited states emitting a burst of photons. The same objective is then used to collect as large a fraction of photons emitted from the focal plane as possible. Only light emanating from the focal plane is transmitted through a micron sized pinhole and detected. Consequently, the transit of the single molecule through the probe volume results in a burst of photons whose size is determined by the fluorescence quantum efficiency and photodegradation rate coefficient of the molecule, the molecular transit time through the detection volume and the optical collection efficiency of the detection system. It should be noted that other less common techniques for single molecule detection in fluids include single-molecule flow cytometry[6–10] and confinement of single molecules in levitated microdroplets.[11,12]

A key benefit of a confocal based approach lies in the ultrasmall detection volumes which greatly reduce the amount of sample needed for analysis when compared to conventional bulk detection methods. However, CFS methods are normally highly wasteful in accessing the entirety of molecular information contained within a given sample. This can be understood by a simple calculation. For a 1 nM solution there is on average less than one molecule resident in a 1 fL probe volume at any given time. If this volume is contained within a microchannel or microwell (with volumes ranging from a few nanoliters to tenths of a microliter) it is clear that detection efficiencies using confocal methods are inherently poor as the majority of molecules will never access the probe volume and therefore will not be detected.

The use of femtoliter probe volumes in single molecule detection is important since background signals originating from Raleigh and Raman scattering by solvent molecules act to reduce signal-to-noise ratios. However, since this background scales proportionally with the probe volume, small probe volumes are effective at minimizing these contributions. This is due to the reduced number of solvent molecules in such small volumes relative to the analyte molecules. Approaches to improving detection efficiencies in single molecule detection experiments have involved the enlargement of the focal region of the laser beam to create a detection

[a)]Electronic mail:a.demello@imperial.ac.uk
[b)]Electronic mail: joshua.edel@imperial.ac.uk

volume in the low picoliter range.[10,13] A primary disadvantage with increasing the detection volume is in the large background signal that arises when the probe volume is enlarged to the picoliter scale. This can often be larger than the fluorescence signal from the target molecule and is directly related to the increase in the number of solvent/impurity molecules in the probe volume.

In capillary-based systems hydrodynamic focusing has been used to narrow the sample stream through use of a sheath flow (orthogonal to excitation).[14,15] This ensures that the entire sample is delivered to the probe region. Under appropriate conditions, each molecule within the sample can be detected sequentially and with high efficiency. This approach is conventionally termed single-molecule flow cytometry (SMFC). In SMFC, individual molecules are motivated within the sample stream at the same rate and experience the same radiation field during their passage through the detection volume. This allows the identification of molecular size on the basis of fluorescence burst characteristics. This approach has been used for DNA fragment sizing,[13] DNA sequencing,[16] and hybridization analysis[17] based on single molecule detection that has been demonstrated and holds great promise for improving sensitivity and reducing analysis times in such assays. However, as previously mentioned, such large probe volumes in single molecule CFS will result in high backgrounds and reduced signal-to-noise ratios. Consequently, a number of methods to suppress background signals have been proposed. These include, pulsed laser excitation coupled with time-gated detection[18] (to discriminate between fluorescence and scattering signals) and photobleaching[19–21] of the sheath flow upstream of the detection volume (to remove the luminescence background from impurity species). More recently, there have been two reports on related methods for improving detection efficiencies in chip-based microfluidic systems. Ho *et al.* used a combination of both hydrodynamic and electrokinetic forces to achieve confinement of small molecules to submicron detection regions within a larger microchannel.[22] Specifically, at a particular location upstream of the detection volume a three-electrode array on the sidewalls and the channel bottom is used to generate electrokinetic forces which are used to steer molecules to a region of minimal energy at the center of the channel. In addition, Stavis *et al.* have reported the fabrication of fluidic channels with submicron (height and width) dimensions.[23] Such systems were used to isolate and detect the binding of single molecules with functionalized quantum dots. Since the detection probe volume is larger than the cross-sectional dimensions of the channel, all molecules theoretically pass through the probe volume and can be detected. Although successful, these methods are complex to implement or require advanced microfabrication facilities. Herein we report the use of hydrodynamic focusing in micron-sized fluidic channels as a route to improving detection efficiency by focusing an analyte stream down to the same order of magnitude as that of the probe volumes used in CFS. Specifically, a single molecule confocal fluorescence detection system is used to probe single microspheres within a hydrodynamically focused analyte stream. Simple statistical methods are subsequently used to investigate the resulting fluorescence bursts and to characterize detection efficiencies. Such an approach is simple to implement and does not require the fabrication of additional elements such as electrodes or submicron diameter channels.

II. EXPERIMENT

A. Instrumentation

Precise details of the experimental system are described elsewhere.[2,3] Briefly, the excitation source used consists of a continuous wave air-cooled multi line argon ion laser operating in light control mode with a wavelength range of 454–514 nm and 7.0 mW (Omnichrome; Melles Griot, Cambridge, UK). The laser beam was spatially filtered (five-axis compact filter; Newport Ltd.) to ensure a near-Gaussian intensity profile as well as expanded by 0.5×. Beamsteering prisms were used to direct the light into the confocal system, with glass neutral density filters attenuating the laser intensity as from 7 mW to 10 μW at the sample. A polarizer was placed prior the prisms in order to control the plane of polarization.

A dichroic mirror (505DRLP02; Omega Optical, Brattleboro, VT) is oriented at 45° to reflect 488 nm radiation and so define a vertical axis, normal to the surface of the optical table. An infinity corrected, high numerical aperture (NA) microscope objective (Fluar 100×/1.3 NA, oil immersion; Carl Zeiss Ltd., Welwyn Garden City, UK) brings the laser light to a tight focus within a microfluidic channel. The collimated laser beam has a $1/e^2$ diameter of 2.5 mm. This was determined by using the knife edge approach. The width is selected to nearly fill the back of the microscope objective, and so yield a beam focus estimated to be close to the diffraction limit. The beam diameter (d) is given by the Eq. (1),

$$d = \frac{1.27\lambda f}{nD}, \tag{1}$$

where D is the incident diameter of the laser radiation at the objective, n is the refractive index of the focusing media, f is the focal length of the objective, and λ is the lasing wavelength. The focused laser spot defines an approximate probe volume of 0.42 fL.

Fluorescence emitted by the sample is collected by the same high NA objective and transmitted through the dichroic mirror. An emission filter (515EFLP; Omega Optical) was placed after the dichroic in order to remove any residual excitation light. A planoconvex lens (+50.2F; Newport Ltd.) focuses the fluorescence onto a precision pinhole ranging in size from 50 μm (Melles Griot) placed immediately in front of a 600 μm fiber optic cable (Elliot Scientific Ltd., UK). The pinhole is positioned in the confocal plane of the microscope objective. This fiber optic cable was coupled directly in front of the detector and adjusted in front of the active area of the detector using a xy stage. The detector is a silicon avalanche photodiode operating in single-photon counting mode (SPCM-AQR-131; EG&G Canada, Vaudreuil, Quebec, Canada). The detector dark count rate on average was approximately 100 Hz. The precision pinhole and fiber optic cable are mounted on XYZ translation stages to allow for fine

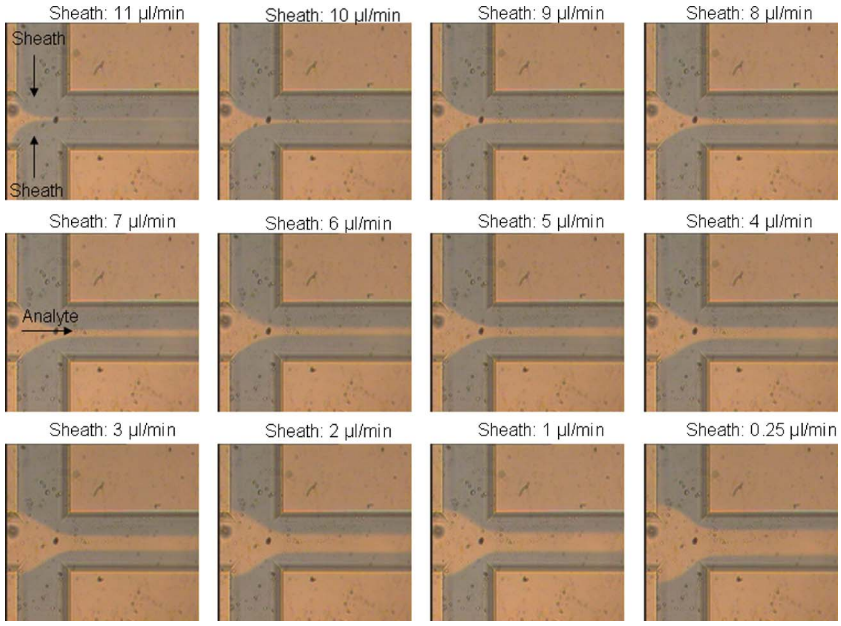

FIG. 1. (Color online) Images of hydrodynamic focusing in a 60 μm wide microfluidic channel. The sheath stream is visualized by dissolving bromthymol blue in water. The analyte flow rate was 5 μl/min and the sheath flow rate was varied between 11 μl/min (top left) to 0.25 μl/min (bottom right).

adjustment of the incoming radiation. The electronic signal from the detector is coupled to a multi channel scalar (MCS-PCI; EG&G), running on a Pentium personal computer.

B. Reagents and chemicals

Fluorescent microbeads (yellow/green Fluospheres®, Molecular Probes; Europe B.V.) having a mean diameter of 0.93 μm were used for the analyte flow in all experiments. Absorption and emission maxima were 505 and 515 nm, respectively. The beads were sonicated for 10 min immediately before use to ensure good dispersion. A working solution of approximately 2.3×10^6 beads/cm^3 was used (effective concentration of 1 μg/cm^3). This is equivalent to a 20 000 fold dilution of the stock solution. All dilutions were performed in tris-borate-EDTA (TBE) buffer. The TBE buffer was prepared at 0.1× concentration [8.9 mM each of tris(methoxy)aminomethane and boric acid, 0.2 mM in ethylenediaminetretraacetic acid; prepared from a solid TBE mixture; Fluka chemical] in a minimum of 18 MΩ deionized water (water purification system, Elga Ltd., Bucks, UK). The sheath flow consisted of a concentrated Bromthymol blue solution and was used for alignment of the analyte flow within the microfluidic channel.

C. Microfabrication and fluidic operation

Glass microfluidic devices were purchased from Micronit (Micronit Microfluidics B.V., Netherlands) and comprised a thermally bonded structured glass substrate containing the microchannel network. Typical channel widths ranged from 20 to 100 μm and had a depth of 30 μm. A simple three inlet 1 outlet channel pattern was designed. The two outer inlets were used for driving the sheath flow while the third central inlet was used for driving the analyte flow. Reservoir access holes (400 μm) were drilled on the top coverplate. The microfluidic chips were further customized in-house by optically polishing the top plate from 1.1 mm down to a thickness of ~150 μm. Optical polishing of the coverplate was performed to reduce the substrate thickness below the working distance of the microscope objective (~170 μm). Finally, 375 μm outer diameter, 150 μm inner diameter polymicrotubing (Composite Metals, Worchester, UK) was glued to the access holes using a chemically resistant glue (Araldite 2014; RS Components, UK). The microchip was placed on a translation stage and appropriately aligned under the microscope objective. Two separate syringe pumps (PHD 2000, Harvard Apparatus, Cambridge, MA) were used to deliver sheath and analyte solutions at various flow rates from 1 ml gastight syringes (Hamilton) into the capillary tubing. Typical flow rates ranged from 0.01 to 20 μL/min.

D. Data analysis

A program written in MATLAB 6.5 (Mathworks, Cambridge, UK) was used to determine peak heights, areas, widths, location as well as for autocorrelation analysis. Briefly, the program searches for a given peak maximum above a specific threshold value which can be defined as three standard deviations from the mean background count rate, i.e., $n_{\text{threshold}}=\mu+3(\mu)^{0.5}$. Adoption of a threshold that lies three standard deviations above the mean yields confidence limits greater than 99%. Once a peak is located, the peak area was determined by analyzing a specified number of bins either side of the peak maximum until the background threshold value is reached. The program then searches for the next peak and continuously repeats until all peaks are accounted for. The mean and standard deviation are then calculated for burst heights, areas, and widths. The distribution plots are histograms generated from all sampled bursts of a given size and flow velocity.

III. RESULTS AND DISCUSSION

Examples of hydrodynamic focusing within the microchannel device can be seen in Fig. 1. Here the analyte flow rate was held constant at 5 μl/min and the sheath flow rates

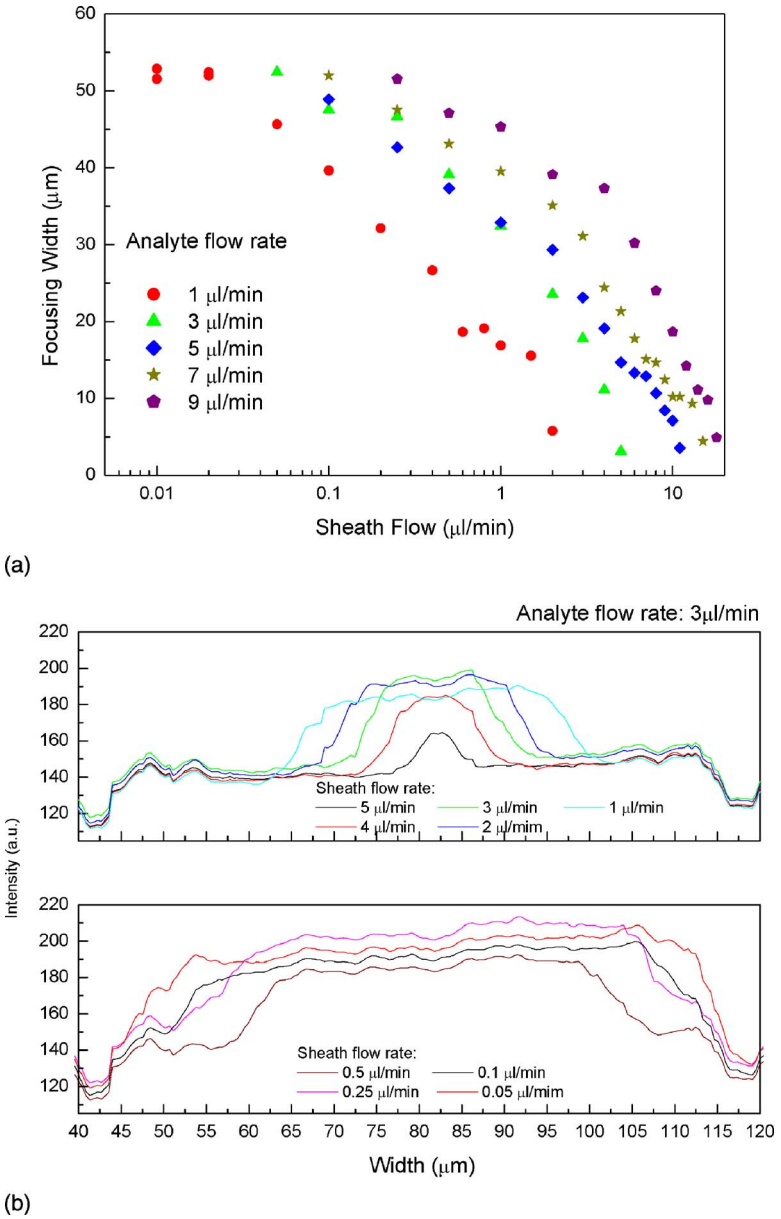

FIG. 2. (Color online) (a) Variation of focusing width as a function of sheath flow rate. Analyte flow rates are 1, 3, 5, 7, 9 μl/min. (b) Focusing cross sections for an analyte flow rate of 3 μl/min at various sheath flow rates.

(blue indicator dye) varied between 11 and 250 μl/min. In the current studies, it is important to operate within a laminar flow regime so that the focused stream will not generate turbulence[24,25] that could result in instabilities in the overall system. Long term stability of the focused streams proved to be good. The analyte stream would remain focused for several hours at a time without any instability in the streams. To achieve long term stability, several factors had to be taken into account. First, the solvents used in the analyte and sheath streams must be well matched in terms of viscosity, density, and solubility. For example, if sheath and analyte streams were made up of organic and aqueous solvents, respectively, instability in the focused stream would occur over long periods primarily due to a mismatch in surface tension between organic and inorganic solvents. Second, identical flow velocities are needed for both sheath streams. If this does not occur, not only will the focused stream be off center within the channel wall but the flow boundary will become unstable. Finally, the microchannels used must have a well defined cross section and have minimal surface related defects.

Figure 2(a) shows focusing widths obtained for various analyte and sheath flow rates. It is interesting to note that all sheath flow rate curves (at a fixed analyte flow rate) follow a similar trend. Maximum focusing was achieved using an analyte flow rate of 3 μl/min and a sheath flow rate of 5 μl/min or an analyte flow rate of 5 μl/min and a sheath flow rate of 10 μl/min. In both instances, a focusing width of approximately 3.8 μl/min was achieved within a 60 μl/min microfluidic channel. In all other cases (i.e., at analyte flow rates of 1, 7, and 9 μl/min) the maximum focusing width was slightly higher at approximately 5 μm. With the microfluidic chip geometry used, the limiting width appears to be just below 1/10th of the channel width. The actual focused width values were determined by importing the raw captured images (as shown in Fig. 1) into MATLAB 6.5 and extracting one-dimensional cross sections. Examples

of this are shown in Fig. 2(b) were the analyte flow rate is kept constant at 3 μl/min and the sheath flow rate varied between 0.05 and 5 μl/min. The stable base line (with an intensity of 140 counts) is due to the sheath and is easily distinguishable from the analyte flow with peak maxima ranging from 160 to 200 counts. The focusing width was determined by the full width half maximum of these cross sections. Inspection of Fig. 2(b) illustrates that the overall symmetry of the focused stream remains constant and is always centered on the central portion of the microfluidic channel. As the sheath flow rate is decreased the focused analyte stream gradually expands in both direction about the central portion of the chip. The channel boundaries are defined by the minima in the cross sections (i.e., 42.5 and 117.5 μm, respectively). This form of symmetry will only take into effect if the conditions discussed in the previous paragraph governing stable hydrodynamic focusing are met.

The focused width is independent of the applied pressure of the sheath stream (i.e., the flow rate). The focusing properties are in fact dependant on the ratio between the sheath and analyte flow rates[26] as shown in Eq. (2),

$$\alpha = \frac{F_s}{F_a}. \tag{2}$$

In this instance F_s is defined as the sheath flow rate and F_a is defined as the analyte flow rate. If α goes below a lower boundary condition $\alpha_{\min}$, the analyte flow rate will take preference and the analyte will go into the sheath flow. Hence, no hydrodynamic focusing will occur. If α goes above an upper boundary condition $\alpha_{\max}$, the sheath flow rate will take preference and the sheath flow will go into the analyte flow. Yet again no focusing will occur. It is therefore essential that in order to achieve hydrodynamic focusing the following condition in Eq. (3) must be met

$$\alpha_{\min} \leq \alpha \leq \alpha_{\max}. \tag{3}$$

$\alpha_{\max}$ and $\alpha_{\min}$ are completely independent of overall flow velocities, but are dependant on the overall dimension and cross section of the microfluidic channel used. In Fig. 3 α is plotted against the focused width. As expected the curve is independent of individual flow velocities as all values of α follow the same curve for a given sheath velocity. From this stability the boundary conditions of α were deduced to be $\alpha_{\min}$=0.014 and $\alpha_{\max}$=2.0. The solid red curve in Fig. 3 is a least square fit to Eq. (4) which is a model proposed by Knight *et al.* describing the focusing width as a function of channel geometry[26]

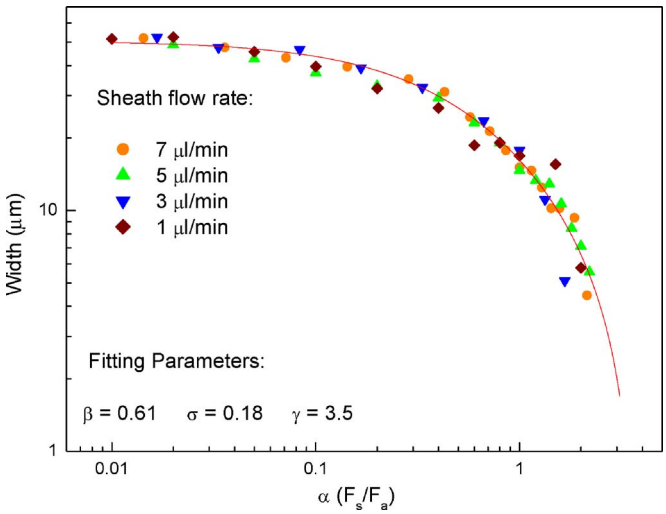

FIG. 3. (Color online) Variation of focusing width as a function of the ratio between sheath and analyte flow velocities. The solid curve is a least-squares fit to Eq. (4).

$$\omega_f = \omega_c \beta \frac{1 + 2\sigma - 2\sigma\alpha}{1 + 2\sigma\gamma\alpha}. \tag{4}$$

Here ω_c is defined to be the channel width, β is a system constant, σ and γ are constants calculated from the expression for the flow rate in a rectangular channel. This equation can only be used if it is assumed that the focused cross section is rectangular in form. The residual in the least-squares fit was 0.985 and, hence, the assumption mentioned before proves to be reasonable.

Fluorescent burst scans from 0.93 μm fluospheres at volumetric flow rates of 50–1000 nL/min have been shown previously by Edel *et al.*[2] using a similar experimental setup without the use of hydrodynamic focusing. Figure 4 shows burst scans for 0.93 fluorospheres at an analyte flow rate of

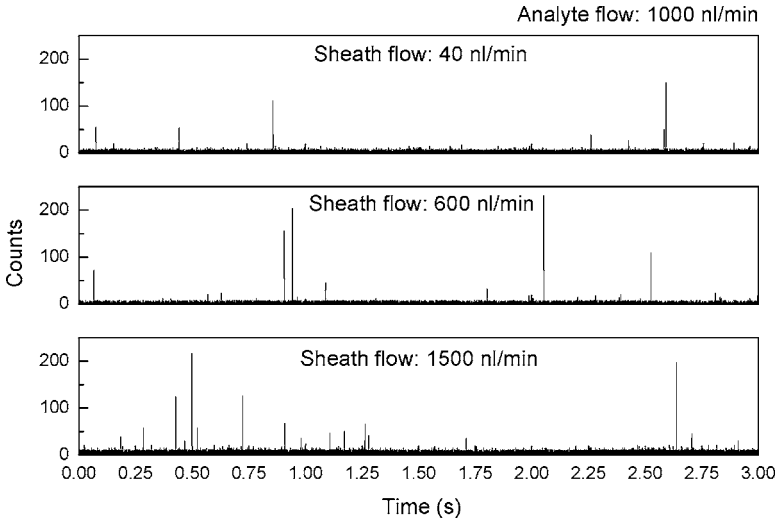

FIG. 4. Burst scans for 0.93 μm fluorescent particles traveling at an initial analyte flow rate of 1 μl/min. The sheath flow velocities are 40, 600, and 1500 nl/min, respectively.

1000 nl/min. The sheath flow rates in Figs. 4(a)–4(c) are 40, 600, and 1500 nl/min. The dwell time in all cases was set to 50 μs to ensure that single particle bursts can be completely resolved and single particle occupancy within the confocal probe volume. Qualitatively, several conclusions can be made. First, the number of single particle bursts detected increases as the sheath flow rate increases. Since the syringe pumps are operating at constant pressure, regardless of sheath flow rate, if the analyte flow velocity remains constant, the same number of fluorescent particles are delivered into the microfluidic channel per unit time. Accordingly an increase in observed bursts is directly related to the focused analyte stream being reduced in width (the focused width to probe volume ratio decreases as the sheath flow is increased). Second, as the sheath flow rate is increased, the individual bursts appear to be more uniform in width. This is primarily caused by a reduction in the range of possible particle trajectories through the probe volume and was observed due to the diffraction-limited focus of the laser beam being approximately three times smaller than the focused width at higher sheath flow rates and 60 times smaller at lower sheath flow rates.

Figure 5 shows the total number of particle bursts detected in a 16 s time interval as a function of sheath velocity. This is shown for analyte flow rates of 1 and 3 μl/min. In both cases the total peaks detected improves by a factor of 10 at the highest sheath flow rates when compared to the respective curve minima. Since the focusing width was negligible at the lowest sheath rates, the total number of peaks detected in these cases is comparable to an unfocused system. Another benefit of hydrodynamically focusing a stream lies in the lower sample consumption that is needed per unit time when compared to a conventionally unfocused approach. This is turn allows for higher throughput relative to sampling time as well as general improvements in the signal relative to background noise. Improving the detection efficiency is crucial in subfemtoliter probe volumes as the majority of molecules or particles surrounding the probe volume can go undetected. Other techniques have been proposed to isolating an analytes trajectory in order to improve detection efficiencies in single molecule studies; however, the dominant trend is to use micro- or even nanochannels ranging from 500 nm to 1 μm. Although this approach ensures the majority of molecules will be detected, severe problems will arise due to channel being plugged due to impurities and analyte crystallization within the channel walls. Hence, ultrasmall channels are not viable for long term or even high throughput measurements. A stable focused flow in microchannels can offer the same degree of improvement in detection efficiencies without the added complexity of nanochannel fabrication and the potential for blocking. The fraction of particles diffusing out of the focused analyte stream into the sheath flow was determined to be negligible for 1000 nm sized particles.

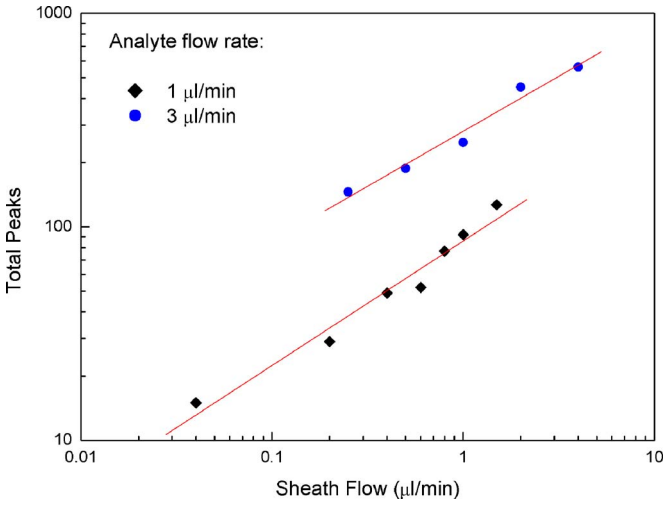

FIG. 5. (Color online) Variation of total particle bursts detected within a 16 s time interval for analyte velocities of 1 and 3 μl/min as a function of sheath flow rate.

A good method to statistically monitor improvements in

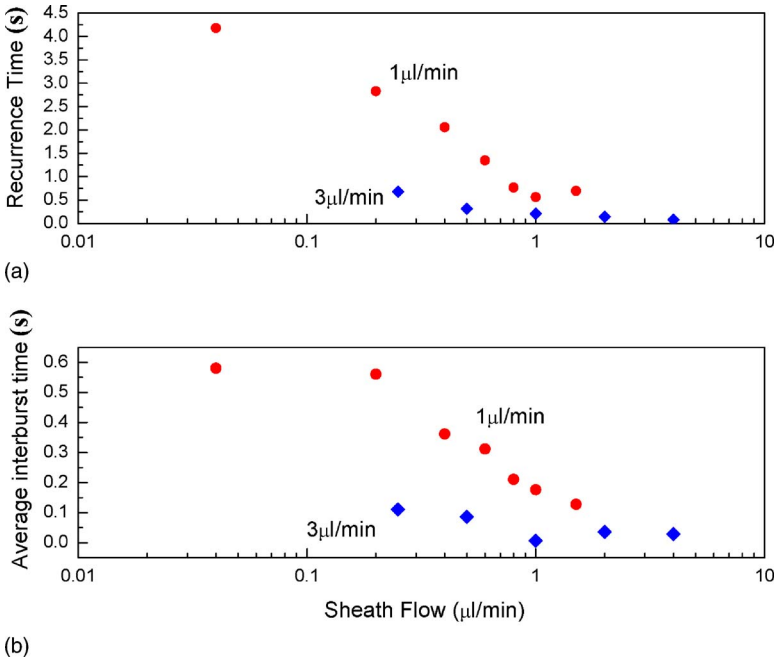

FIG. 6. (Color online) (a) Variation of recurrence time for analyte velocities of 1 and 3 μl/min as a function of sheath flow rate. (b) Variation of average interburst time for analyte velocities of 1 and 3 μl/min as a function of sheath flow rate.

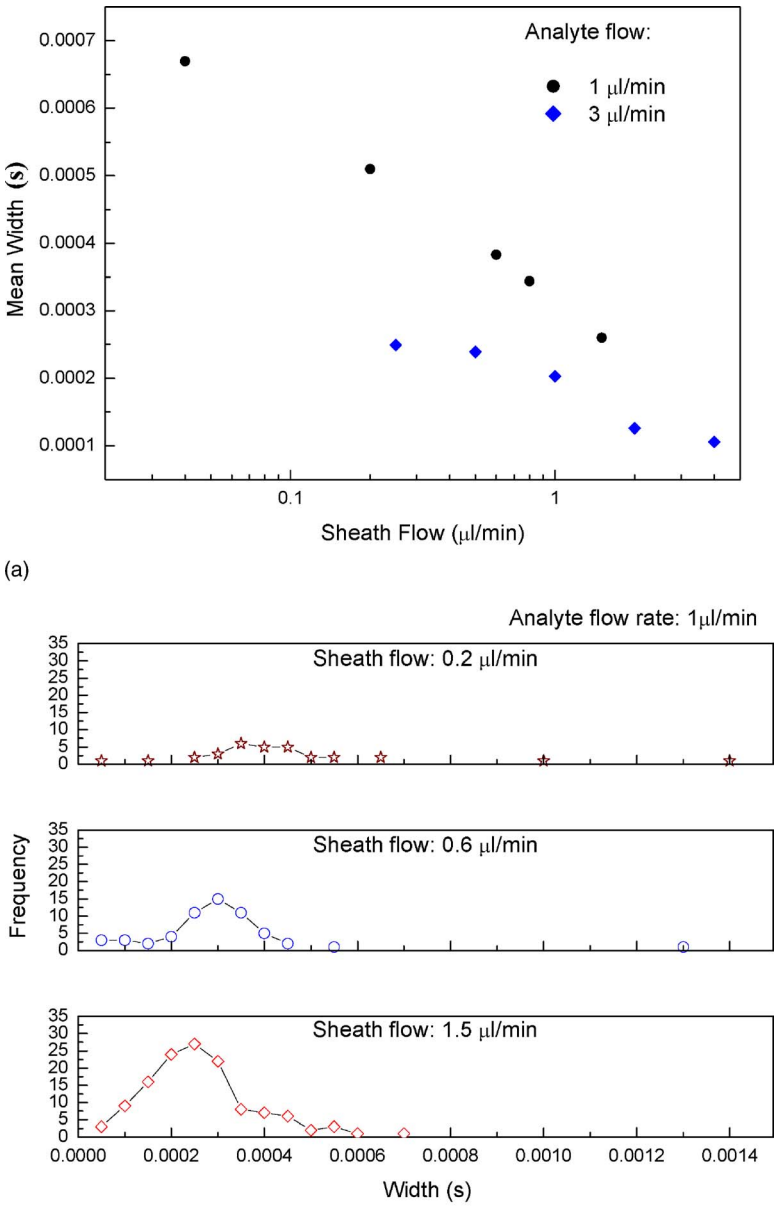

FIG. 7. (Color online) (a) Variation of mean burst width as a function of sheath flow rate for analyte flow velocities of 1 and 3 μl/min. (b) Histogram of particle width distributions for an analyte flow rate of 1 μl/min and sheath flow rates of 0.2, 0.6, and 1.5 μl/min, respectively.

detection efficiencies is by calculating recurrence times. This approach relies on the use of Poisson statistics. Burst interval distributions are predicted to follow a Poissonian model, in which peak separation frequencies adopt an exponential form. The probability of a single molecule (or particle) event occurring after an interval Δt is given by Eq. (5),

$$N(\Delta t) = \lambda \exp(-\beta \Delta t), \tag{5}$$

where λ is a proportionality constant and β is a characteristic frequency at which single molecule events occur. The recurrence time τ_R can then be simply defined as

$$\tau_R = \frac{1}{\beta}. \tag{6}$$

Equation (5) simply states that longer intervals between photon bursts are less probable than shorter intervals at a given sheath flow rate. It is also expected that τ_R should be inversely proportional to concentration, sheath flow rate (at a constant analyte flow) or solvent viscosity in a range of systems. Figure 6(a) shows frequency $N(\Delta t)$ versus time plots for two analyte flow rates as a function of sheath flow. In both cases the recurrence times between events decreases by a factor of 10 between bursts in an unfocused stream and in a highly focused stream. This clearly supports the data shown in Fig. 5 and demonstrates that a tenfold improvement in detection efficiency is achievable.

Figure 6(b) illustrates a simpler analysis of event frequency. In this case the total number of fluorescent bursts counted at a given flow rate and time interval are taken into account. From this the average interburst time (AIT) can be deduced. Figure 6(b) shows plots of average interburst time versus sheath flow rate. As with the Poisson recurrence times, the AIT also decreases by the same order of magnitude as the sheath flow rate was increased.

One of the potential downsides of hydrodynamically focusing analyte flows lies in the linear velocity of the focused stream increasing and, hence, causing the particles burst width to decrease as the sheath flow is increased. This effect

can be seen in Fig. 7(a). For example, at an analyte flow rate of 1 μl/min and a sheath flow rate of 40 nl/min, the average burst width was measured to be 670 μs. When a sheath flow rate of 1.5 μl/min is used the average burst width decreases further to 260 μs. At an analyte flow rate of 3 μl/min and a sheath flow rate of 250 nl/min, the average burst width in this case was 249 μs. When a sheath flow rate of 4 μl/min was used the average burst width decreases to 109 μs. It is therefore crucial to have relatively low dwell times (10 $-$50 μs) to obtain statistically reliable information regarding the burst distributions. The downside can be overcome by simply using a multichannel scalar capable of submillisecond dwell times.

A clear benefit in minimizing the focused analyte stream width is seen in Fig. 7(b). A histogram of burst width distributions is plotted for an analyte flow velocity of 1 μl/min and sheath flow rates of 0.2, 0.6, and 1.5 μl/min. The average peaks width in each case was 510, 383, and 260 μs, respectively. Not only does the average burst width decrease with time but the overall distribution sharpens with increased sheath flow. In addition, the full width half maximum in the distributions decreases with increased sheath flow. This can be better determined from the decrease in relative standard deviations in the burst widths. They are 48%, 41%, and 35%, respectively. Another benefit of focusing can be seen in the width distribution maxima. At a sheath flow rate of 1.5 μl/min the distribution maximum occurs at 250 μs with a count rate of 27 counts. This is much higher than for a sheath flow rate of 0.2 μl/min where a distribution maximum was recorded at 350 μs with only six counts.

IV. CONCLUSIONS

The studies herein define a novel approach to improving detection efficiencies in subfemtoliter probe volumes using confocal spectroscopy. This was achieved by hydrodynamically focusing an analyte stream within a microstructured channel so that the analyte stream width would be comparable to that of the probe volume. With this approach a tenfold increase in the relative detection efficiency can be achieved without the addition of active focusing components. Statistical analyses of the results also demonstrate significant improvement in the burst width distributions when the analyte stream width is minimized. Using the current approach to analyte stream focusing obviates the need for the fabrication of high cost nanochannels or integrated electrode arrays to improve detection efficiencies. More importantly, the technology described is simple to implement and easy to control. In fact we expect the approaches can be utilized in the future for experiments such as single cell counting and sorting as cell dimensions tend to be larger than the minimum focusing width achieved. These studies and other are currently underway and will be reported in future publications.

[1] Y. Ishii and T. Yanagida, Single Mol. **1**, 5 (2000).
[2] J. B. Edel, E. K. Hill, and A. J. de Mello, Analyst **126**, 1953 (2001).
[3] E. K. Hill and A. J. de Mello, Analyst **125**, 1033 (2000).
[4] S. M. Nie, D. T. Chiu, and R. N. Zare, Anal. Chem. **67**, 2849 (1995).
[5] M. A. Osborne, S. Balasubramanian, W. S. Furey, and D. Klenerman, J. Phys. Chem. B **102**, 3160 (1998).
[6] A. Agronskaia, J. M. Schins, B. G. de Grooth, and J. Greve, Anal. Chem. **71**, 4684 (1999).
[7] R. M. P. Doornbos, B. G. de Grooth, and J. Greve, Cytometry **29**, 204 (1997).
[8] M. M. Ferris and K. L. Rowlen, Rev. Sci. Instrum. **73**, 2404 (2002).
[9] P. M. Goodwin, W. P. Ambrose, J. C. Martin, and R. A. Keller, Cytometry **21**, 133 (1995).
[10] X. Yan, W. K. Grace, T. M. Yoshida, R. C. Habbersett, N. Velappan, J. H. Jett, R. A. Keller, and B. L. Marrone, Anal. Chem. **71**, 5470 (1999).
[11] J. M. Ramsey and W. B. Whitten, Abstr. Pap. - Am. Chem. Soc. **199**, 62 (1990).
[12] W. B. Whitten, J. M. Ramsey, S. Arnold, and B. V. Bronk, Anal. Chem. **63**, 1027 (1991).
[13] A. van Orden, R. A. Keller, and W. P. Ambrose, Anal. Chem. **72**, 37 (2000).
[14] J. N. Demas, M. Wu, P. M. Goodwin, R. L. Affleck, and R. A. Keller, Appl. Spectrosc. **52**, 755 (1998).
[15] D. C. Nguyen, R. A. Keller, J. H. Jett, and J. C. Martin, Anal. Chem. **59**, 2158 (1987).
[16] P. M. Goodwin *et al.*, Exp. Tech. Phys. (Lemgo, Ger.) **41**, 279 (1995).
[17] C. Y. Zhang, S. Y. Chao, and T. H. Wang, Analyst **130**, 483 (2005).
[18] S. A. Soper, R. A. Keller, E. B. Shera, J. C. Martin, and J. H. Jett, Abstr. Pap. - Am. Chem. Soc. **200**, 135 (1990).
[19] R. L. Affleck, W. P. Ambrose, J. N. Demas, P. M. Goodwin, and R. A. Keller, Anal. Chem. **68**, 2270 (1996).
[20] R. L. Affleck, W. P. Ambrose, J. N. Demas, P. M. Goodwin, J. A. Schecker, J. M. Wu, and R. A. Keller, Anal. Chem. **68**, 2270 (1996).
[21] C. Eggeling, J. Widengren, R. Rigler, and C. A. M. Seidel, Anal. Chem. **70**, 2651 (1998).
[22] T. H. Wang, Y. H. Peng, C. Y. Zhang, P. K. Wong, and C. M. Ho, J. Am. Chem. Soc. **127**, 5354 (2005).
[23] S. M. Stavis, J. B. Edel, K. T. Samiee, and H. G. Craighead, Lab Chip **5**, 337 (2005).
[24] I. Papautsky, J. Brazzle, T. Ameel, and A. B. Frazier, Sens. Actuators, A **73**, 101 (1999).
[25] F. G. Bessoth, A. J. de Mello, and A. Manz, Anal. Commun. **36**, 213 (1999).
[26] J. B. Knight, A. Vishwanath, J. P. Brody, and R. H. Austin, Phys. Rev. Lett. **80**, 3863 (1998).